LINarm++

Affordable and Advanced LINear device for ARM rehabilitation

Deliverable D4.1

Proof-of-concept system for principles of user state assessment and design of sensory system

Contractual delivery date	31.10.2015 (month 6)
Actual delivery date	31.10.2015 (month 6)
Version	1.0
Dissemination level	CO
Authors	Matjaž Mihelj (UL) Janez Podobnik (UL) Jure Pašić (UL) Blaž Jakopin (UL)

Contents

Executive summary 2
Introduction..... 3
LINarm robot and sensor integration..... 4
Technological challenges..... 5
Proof-of-concept robot and sensory system..... 6
HapticMaster robot and display..... 6
Physiological sensors of the reference measurement system..... 7
Measurements of the physiological response during the rehabilitation training 8
Development of the measurement system 8
Measurements of the skin conductance..... 9
Measuring the heart rate 12
Measuring the skin temperature 15
Sensor integration 17
Experiments..... 18
Signal preprocessing and feature extraction 21
Electrocardiogram (ECG) 21
Photoplethysmography (PPG) 22
Skin conductance 24
Peripheral skin temperature 25
Results 27
Changes in physiological signals during exercise 27
Comparison between different measurement systems 28
Conclusions..... 34
Literature on physiological sensors and sensor signal processing..... 35

Executive summary

This deliverable deals with a proof-of-concept system for acquisition of data required for developing and testing the patient model. The proof-of-concept system consists of state-of-the-art equipment already available at UL (g.USBamp biosignal amplifier and sensors for measuring physiological and physical parameters, HapticMaster robot with a force sensor, wireless IMU sensors). Experiments serve to a) acquire a set of measurements to test the patient model, b) determine, test and verify the configuration of embedded-and-wearable sensory system and c) develop and verify training scenarios for the LINarm++ system. In addition to the proof-of-concept system several prototypes of embedded sensory system were developed and their performance compared to the reference sensory system. Healthy subjects were involved in preliminary pilot trials with the proposed setup.

Introduction

Rehabilitation robots are devices that assist the recovery of patients whose motor functions are impaired as a result of stroke, spinal cord injury or other condition. Their benefit is twofold. First, they offer accurate sensors for measurement of forces and positions, thus providing a method of objectively evaluating the patient's motor performance. Second, robots with active motors can help the patient train simple or complex movements, taking some of the strain off therapists. Training with such robots yields long-term results comparable to exercise with a therapist. Frequently, they are combined with virtual environments in order to make rehabilitation more interesting and motivational.

Several rehabilitation systems based on different robots were developed, such as the MIT-Manus, a 2-degree-of-freedom system that supports planar movements using an impedance controller, the GENTLE/s based on the HapticMaster robot or the ARMin. However, while early rehabilitation robots were able to provide active assistance to the patient, they did not adapt their movement to the activity (or passivity) of the patient. Rather, the affected limb was moved along a predefined, fixed trajectory. The patient was also not informed about his or her activity and contribution to the movement. This problem was addressed by patient-cooperative or "assist as needed" control techniques. By recognizing the patient's movement intentions and motor abilities, patient-cooperative techniques adapt the robotic assistance to the activity (or passivity) of the patient. Recently, the concept of patient-cooperative robotics has been extended to biocooperative robotics within the MIMICS EU project, which take into account not only the bidirectional flow of energy between the patient and the robot, but also psychophysiological factors. In a biocooperative rehabilitation task, the parameters of the task are automatically adjusted so that the patient is challenged in a moderate but engaging and motivating way without causing undue stress or harm. The implementation of biocooperative control within the MIMICS project was relatively cumbersome with physiological sensors attached to the patient's body. At the same time psychological state was found challenging to estimate. However, physiological responses still provided an important insight into patient's state during the training.

Within the LINarm++ project the main focus will be on the development of unobtrusive sensing technologies for measurement of physiological responses of patients during training with the robot and the use of this information to adapt the training program. Control of a robotic device relies on high quality measurements. At the same time quality of rehabilitation depends on good assessment of patient's performance and adaptation of the training protocol to the patient's needs. The most relevant physiological parameters to be measured are (at least a subset of the following measurements will be implemented in the LINarm++): 1) heartrate, 2) galvanic skin response (skin conductance), 3) skin temperature (at the finger or similar location), 4) electromyography of arm muscles to provide more insight into the subject's voluntary physical activity, 5) breathing frequency (not easily measured without obtrusive sensors – chest belt or thermistor under the nose).

LINarm robot and sensor integration

The LINarm robot is an assistive device for the rehabilitation of the upper limb, specifically designed to minimize the overall realization costs to enable rehabilitation exercises at home. It features a variable stiffness mechanism, making it possible to adjust the level of assistance by modifying the manipulandum mechanical stiffness on the basis of the actual requirements of the therapy.

The sensor setup needs to be low-cost and unobtrusive. Therefore, most of the sensors should be embedded directly into the robot mechanism or simply attached to the patient (e.g. bracelets). Sensors embedded in the robot itself already provide information about the arm (hand) position, velocity and interaction force (including grasping force) between the robot and the patient. The acquired information can provide an insight into the physical interaction between the robot and the patient (supporting forces, exchange of power).

The interface between the patient and the robot is the handle that provides the most suitable location for integration of physiological sensors (Figure 1). In this way the patient would not be disturbed by the measurement procedure.

The robot measurement system can also be augmented with simple wearable sensors attached to the patient to complement information from the embedded sensors in the robot itself. The wearable sensory system consists of magneto-inertial, small, lightweight, wireless and battery powered devices that allow natural human movements. The output of the system would be a complete kinematic model of the upper limb that includes shoulder and elbow angles (can be used to properly activate electrical stimulation).

All sensors must be interfaced to the control computer. Sensors signals must be processed on a low cost hardware meaning that complexity of processing algorithms needs to be limited. The sensors outputs will be used as the input into the patient’s model (together with kinetic and kinematic measurements).

Figure 1 LINarm device with the handle as the main interface between the robot and the patient

Technological challenges

The integration of physiological sensors within the handle results in various technological challenges related to non-static measurement conditions. Sensory system and its output might be influenced by artefacts resulting from arm movement. Patient's grasping force on the handle changes during training, arm configuration changes due to robot movements and contact area between the hand and the handle is not constant. At the same time the handle needs to be ergonomically designed and should fit to patients with various hand sizes. Also sterilization of the robot handle and embedded sensors should be considered. The problem is less critical for home use and more critical for clinical use.

As an alternative to putting physiological sensors into the robot handle the following solutions can be considered: 1) bracelet with embedded sensors (battery powered and wireless – certain modern wrist watches use this concept), 2) measurements conducted on the resting arm (sensors embedded into a form of handle or another approach can be considered), 3) bimanual measurement of physiological signals (heartrate can be measured as in the fitness devices).

In order to validate these challenging conditions a proof-of-concept system was developed to test and validate possible measurement technologies before making the final decision about sensor integration.

Proof-of-concept robot and sensory system

The proof-of-concept system is a complete rehabilitation device with the robot and all sensing modalities presented in the Introduction chapter. The main differences in relation to the final LINarm solution are: HapticMaster robot to emulate the LINarm device, a reference state-of-the-art sensory system for measuring physiological responses, various implementations (prototypes) of low-cost embedded-and-wearable sensory system and the training task adapted for use with healthy subjects (for validation sensory system patients' involvement is note necessary).

HapticMaster robot and display

The HapticMaster robot, developed by Moog FCS, was used as the haptic interface. Shown in Figure 2, this robot has three degrees of freedom. The first joint represents vertical translation, the second rotation around a vertical axis, while the third allows horizontal translation. The robot's end-effector also contains a three-axis force sensor.

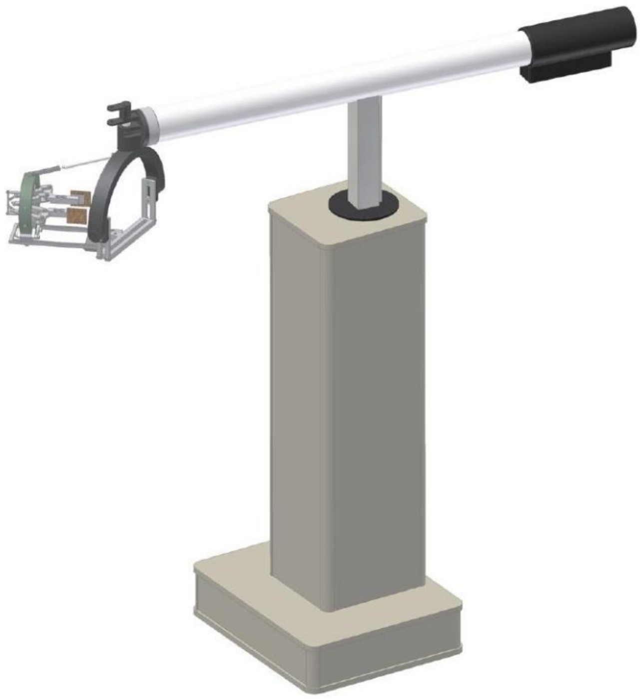

Figure 2 The HapticMaster robot

The HapticMaster has previously been used in the GENTLE/s and MIMICS rehabilitation platforms and can thus be considered a suitable choice for robot-aided upper extremity rehabilitation.

While the robot has three degrees-of-freedom, only one translational degree-of-freedom is required to emulate the LINarm device. Therefore, the vertical translational and the rotational degree-of-freedom were controlled in a predefined position, only the horizontal axis was used to simulate the LINarm movement.

A 1.2x1.2-meter screen was used to display visual data. Subjects sat approximately 2 meters in front of the screen, with the robot situated between the seat and the screen.

Physiological sensors of the reference measurement system

Three primary physiological measurements were chosen: electrocardiography, skin conductance, and peripheral skin temperature. A fourth possible measurement would be the respiration rate, however, as it cannot be measured completely unobtrusively (sensor needs to be attached to the patient), it was omitted.

All reference physiological sensors were manufactured by g.tec (Graz, Austria). Skin temperature and skin conductance sensors are shown in Figure 3. The electrocardiogram (ECG) was recorded using four disposable surface electrodes placed in the following configuration: one electrode on the left part of the chest, one on the right part of the chest, one on the left part of the abdomen, and a ground electrode on the upper left part of the back. Skin conductance was measured using a g.GSR sensor. The electrodes were placed on the distal phalanxes of the second and third fingers of the resting hand. The sensor generated a constant voltage between the two electrodes and measured the current between the electrodes in order to estimate skin conductance according to an established procedure. Peripheral skin temperature was measured using a g.TEMP sensor attached to the distal phalanx of the fifth finger of the resting hand. All of these signals were connected to a g.USBamp signal amplifier (Figure 4). The sampling frequency was 1.2 kHz. Skin conductance and skin temperature can all be accurately measured with a much lower sampling frequency (below 20 Hz) while a recommended ECG sampling frequency that allows accurate analysis of heart rate variability is approximately 500 Hz.

Figure 3 Physiological sensors: temperature (left) and skin conductance (right). All manufactured by g.tec.

Figure 4 The g.USBamp signal amplifier (manufactured by g.tec).

Measurements of the physiological response during the rehabilitation training

Laboratory and clinical environment permits well-controlled measurements of physiological parameters. However, at home the user is usually not helped by the physiotherapist or healthcare giver, who would attach sensors properly and check constantly if the sensors are working properly. The question which needs to be addressed for home use is how to ensure good and sufficient quality of measuring the physiological parameters during the rehabilitation training at home.

For the purpose of measuring the physiological parameters at home we have developed several measurement systems, which consist of low-cost sensors for measuring physiological parameters. Most importantly the measurement systems are designed in such a way that they do not need to be attached to the user and therefore do not need instructions, and in best case the user will not even need to be aware of the sensors. Sensors were integrated into the handle, which is the interaction point (sometimes also attachment point if user's hand needs to fixated to the robot) between the user and the training device. Two handles were tested: the handle in shape of cylinder, and the handle in shape of a half of the sphere. The third system was wearable measurement system attached to the wrist.

Development of the measurement system

Full experimental measurement system setup consists of two types of handles (cylindrical and spherical), which are attached to the robot, one wearable bracelet and reference measurement system. Figure 5 shows the experimental setup.

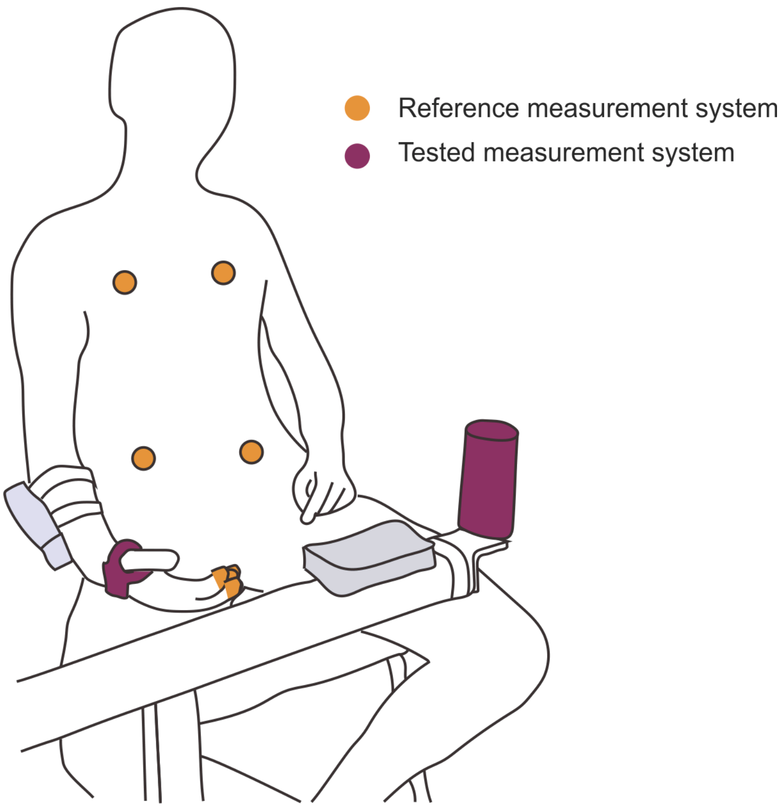

Figure 5 Sensors attachment points of the measurement systems

Measurements of the skin conductance

To measure the conductivity of the skin we used standard dry AgCl electrodes with a contact area of about 1cm2, as suggested by the literature [20, 21]. As previously mentioned the problem of measuring skin conductance is wide measurement range needed to measure a conductance of the skin, since different users have largely different levels of skin conductance. We tested two versions of the amplifiers (shown in Figure 6):

- basic non-inverting amplifier,
- nonlinear adaptive amplifier (proposed in [20]).

Signals from both amplifiers was sampled with 12 bit analog-to-digital converter with sampling frequency of 100 Hz. Synchronized measurements from both amplifiers are presented in Figure 7.

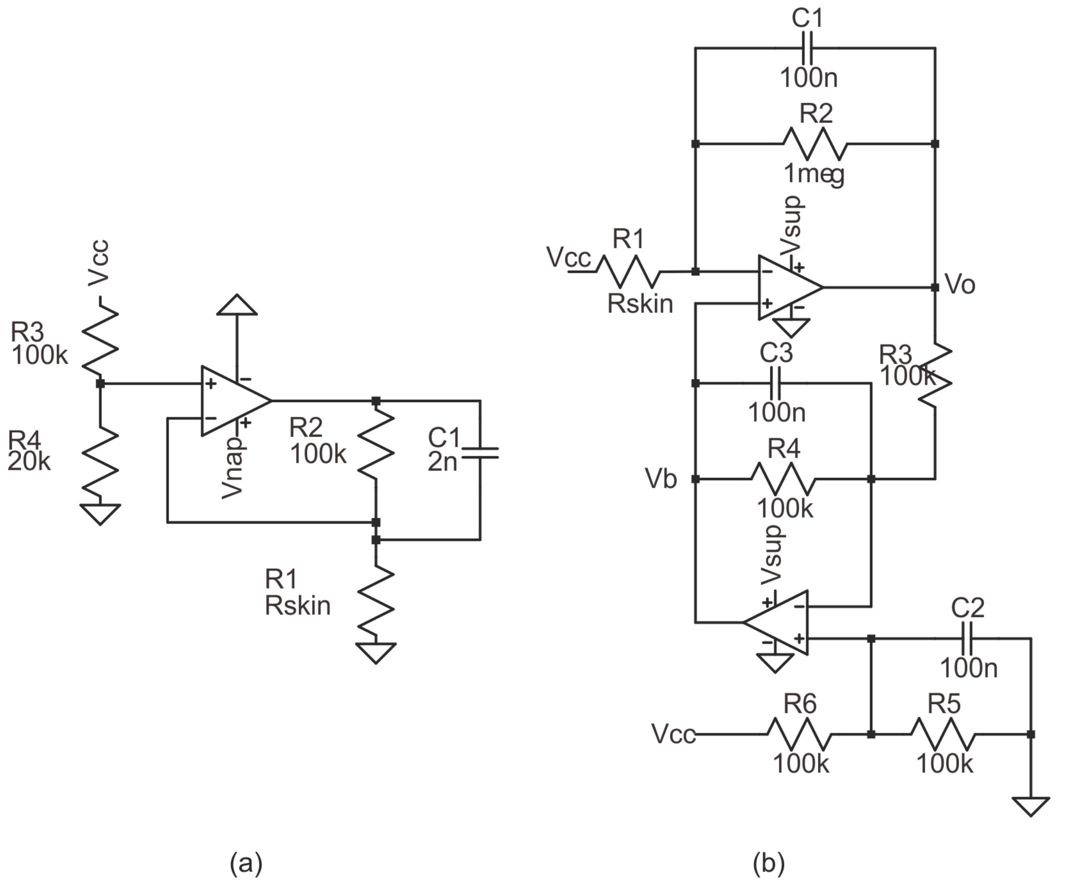

Figure 6 Two versions of tested amplifiers: (a) basic non-inverting amplifier and (b) non-linear amplifier with feedback loop.

The response of the first amplifier was calculated using the equation of the amplification of the amplifier $V_O = (1 + \frac{R_2}{R_{skin}})V_{CC}$. Conductance as an inverse of the resistance was determined by expressing the resistance of the skin from above equation:

$$R_{skin} = R_2 \frac{0.5}{V_O - 0.5}$$

The final skin conductance is given by $G_{skin} = \frac{1}{R_{skin}}$.

Skin conductance when using the second (nonlinear) amplifier was calculated using the equation

$R_{skin} = 10^6 \frac{V_O}{3-2V_O}$,

and the final conductance is again the inverse of the resistance $G_{skin} = \frac{1}{R_{skin}}$.

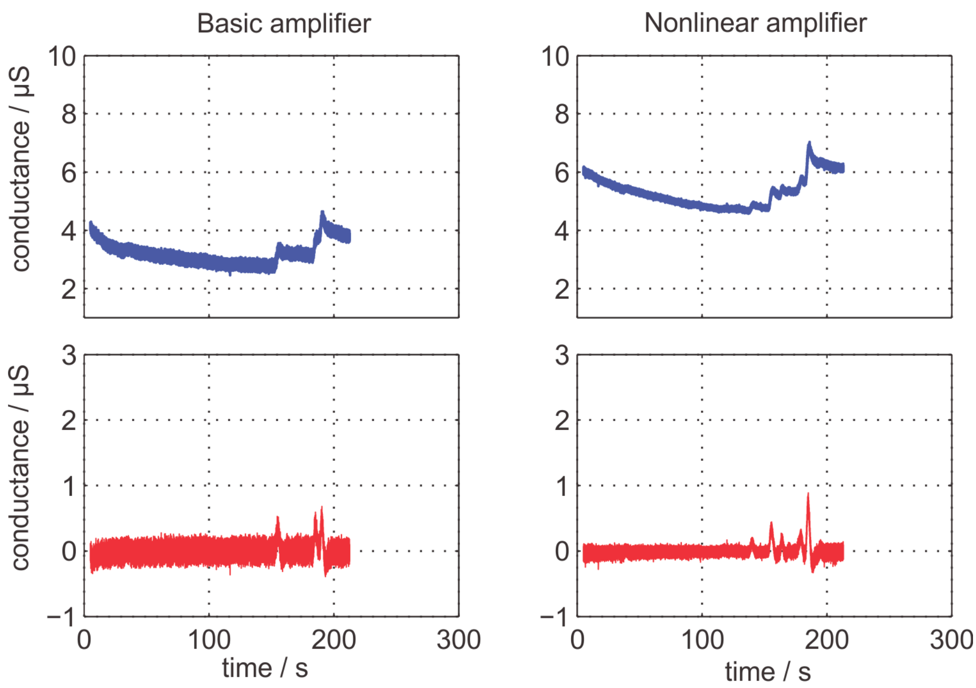

Figure 7 Comparison of the response of the amplifiers.

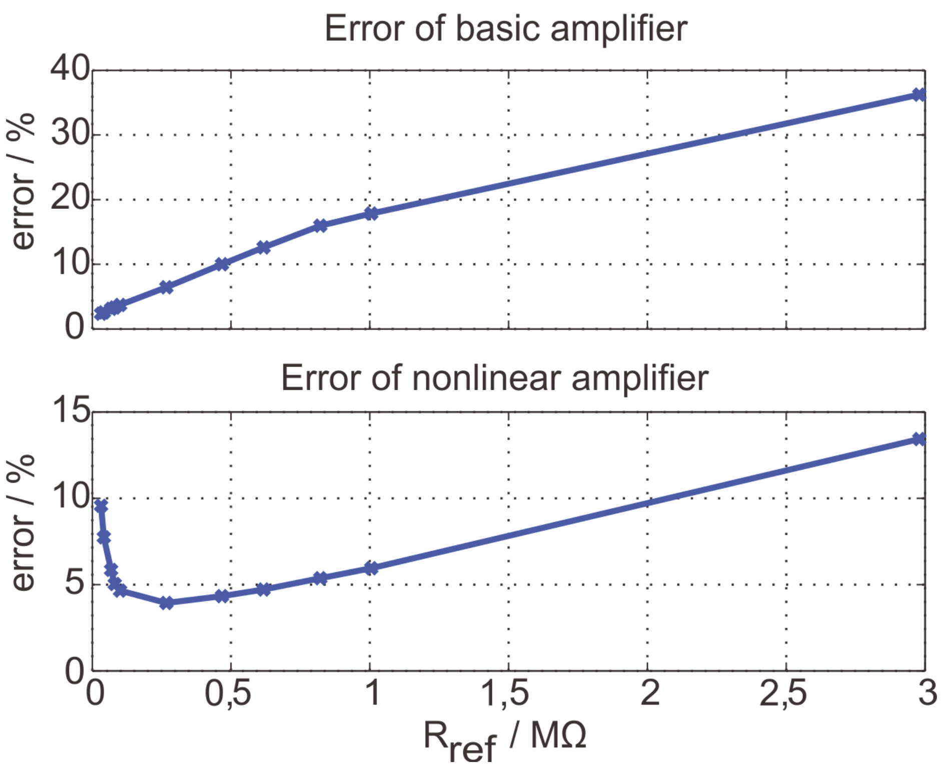

Figure 8 Errors of the amplifiers.

From the figures it can be seen that the nonlinear amplifier has better signal-to-noise ratio, which was additionally supported with additional measurements on a wide range of tested conductance levels corresponding to expected conductance levels of human skin. Figure 8 shows the results. Based on presented results the nonlinear amplifier was chosen as an appropriate solution for amplifying the signals for measuring the skin conductance.

Measuring the heart rate

For the measurements of the heart rate we chose Pulse Sensor, which is a low-cost solution for pulse photopletismography measurements, which uses only one light source and is based on a reflective method. The sensor is easy to use from the ergonomic point of view, however due to its high susceptibility to movements, which result in movement artefacts, and high sensitivity to outside lighting; it works well only under well controlled conditions. Analog signal from the sensors was sampled with 12 bit analog-to-digital converter with sampling frequency of 100 Hz. Figure 9 shows the sensor.

(a) (b)

Figure 9 Pulse sensor: (a) front of the sensor with light source and detector, (b) back of the sensor with SMD elements.

Heart rate and heart rate variability provide valuable information about user's health and physiological state. Since above mentioned parameters can easily be extracted from a simple electrocardiogram (ECG) signal, ECG monitor is a good candidate to be embedded into our system.

Heart rate measurement begins with acquisition of the ECG signal through a set of skin electrodes, mounted on the user's chest. They are in most cases adhesive gelled stickers but in our case, due to more convenient use, we use gel-les electrodes mounted directly on both handles. Acquired signal has low power and it is very prone to different kinds of noise. Therefore a specialized ECG amplifier is used to isolate the heart beat signal from the noise and prepares it for further hardware filtering and software heart rate and variability extraction. Signal routing diagram can be seen on the Figure 10.

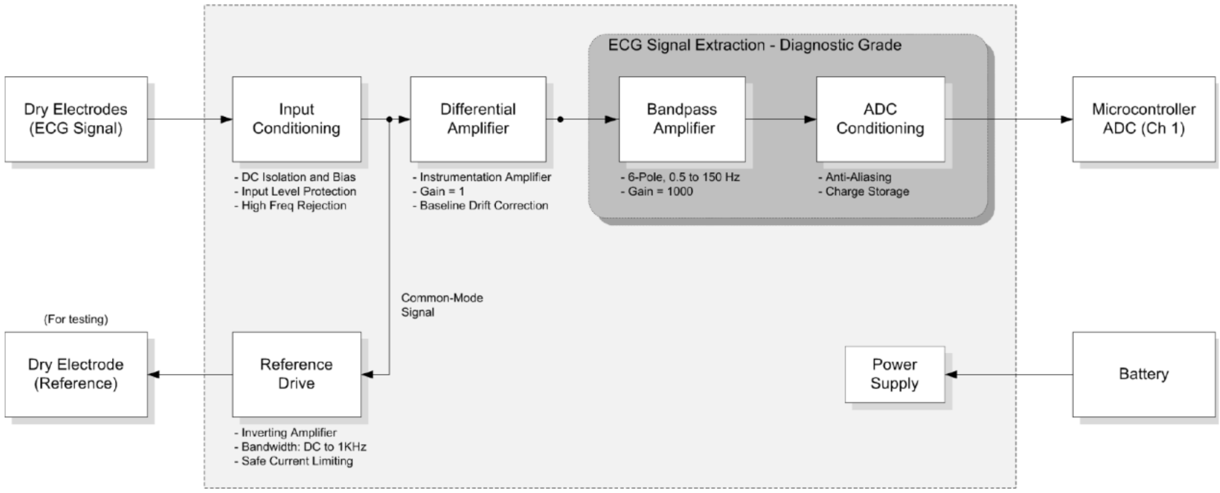

Figure 10 ECG signal routing diagram

ECG monitor circuit (Figure 11) consists of several parts, each one handling its own task. Resistors at the input of the circuit are protecting the subject from too high current from it while capacitors protect the amplifier from unbalanced input signal. Reference drive is holding the subject on constant DC level in order to balance input signal DC level, which further improves the stability of the output signal. Amplifiers and filters after the instrumentation amplifier are stabilizing and filtering the signal against high frequency noise and low frequency drifting. Finally, power supply part is in charge of producing bipolar voltage and driven ground out of a single battery cell.

Hardware signal filtering has been made of low pass filter with the cut off frequency of 30Hz and high pass filter with the cut off frequency of 5Hz. Values were empirically tested and are slightly deviating from the proposed American Heart Association requirements for electrocardiographic equipment (160Hz and 0.5Hz).

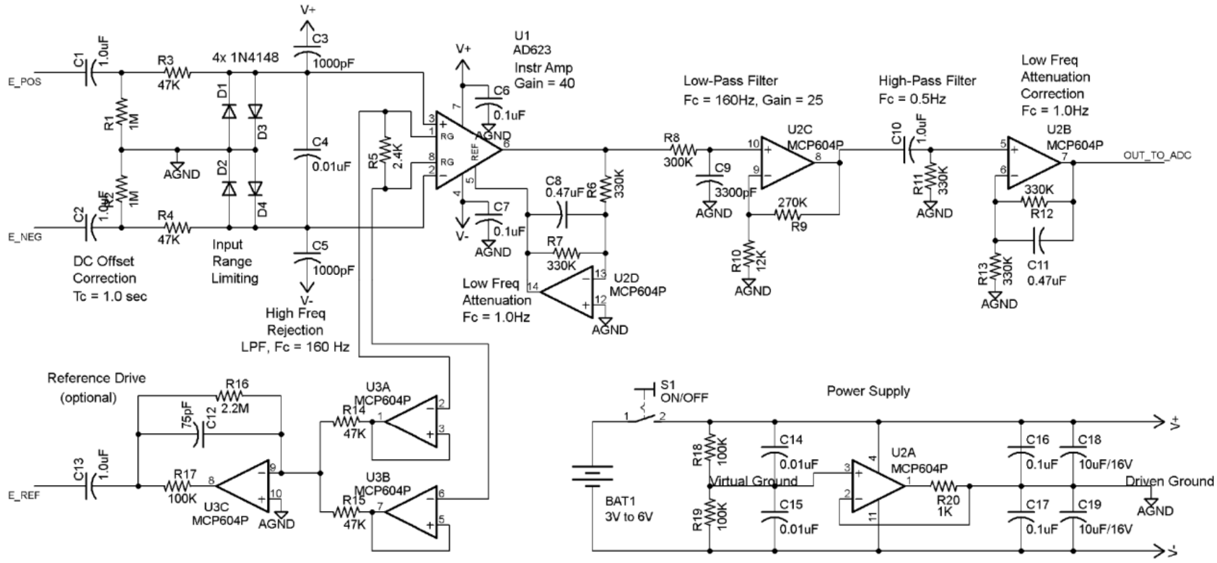

Figure 11 ECG circuit schematics

Our ECG monitor was firstly compared to the commercially available medical monitor. Both were connected to the subject with commercial adhesive gelled electrodes. Figure 12 is showing signals from both units. Blue line presents the reference system output, red one our ECG monitor without reference signal, and black one with the reference signal.

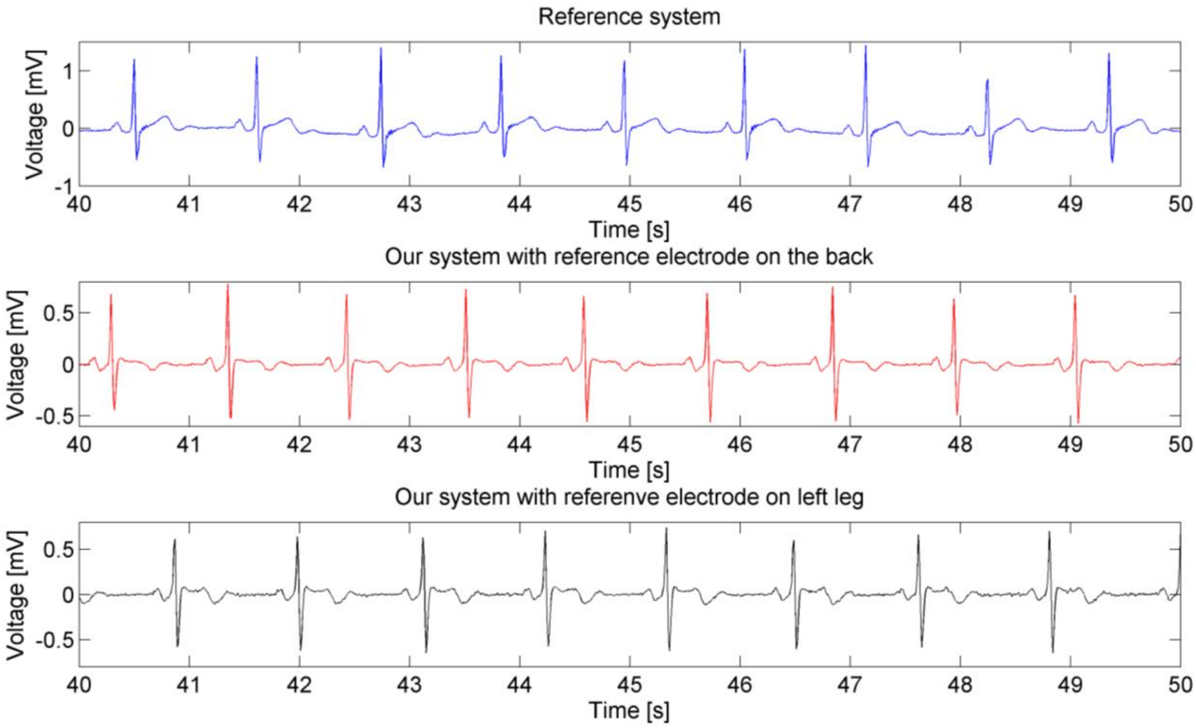

Figure 12 Comparison between medical equipment and our ECG monitor

After satisfactory results a simplification and more user friendly upgrades has been made regarding electrodes. Since adhesive stickers are not so convenient for our type of application, gel-less hand hold electrodes were tested. Output signal is much more noisy but still very usable in our case. On Figure 13 a comparison between reference system and our gel-less electrode ECG monitor is presented.

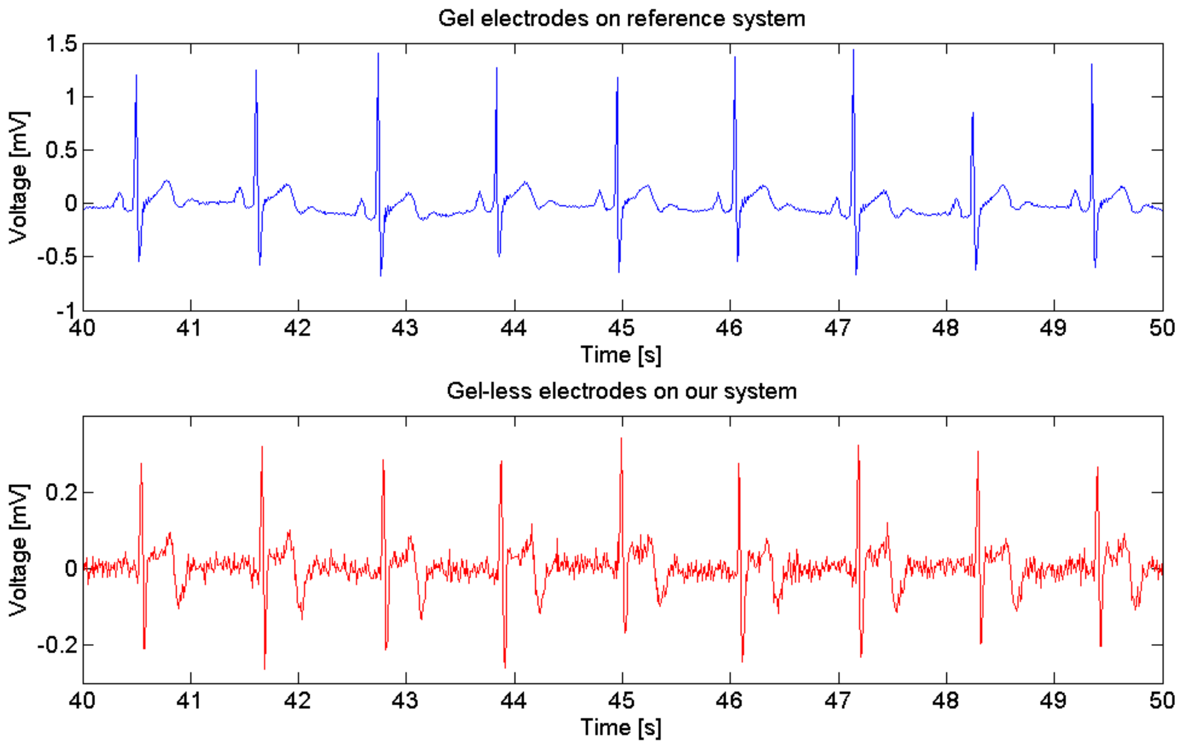

Figure 13 Comparison between reference system and our gel-less electrode ECG monitor

Measuring the skin temperature

To measure the skin temperature we chose NTC thermistors due to its fast response and ease of use. We compared several thermistors. We tested a thermistor enclosed in housing (commercial medical thermistor), thermistor in bare SMD housing (ERTJ1VS104FA Panasonic) and a thermistor in a vacuum glass flask (62S3KF354G Belatherm). Thermistors are shown in Figure 14. Resistance of thermistors was measured using a bridge circuit. The changes in voltage potentials of the bridge circuit were measured using linear amplifier and an analog to digital converter.

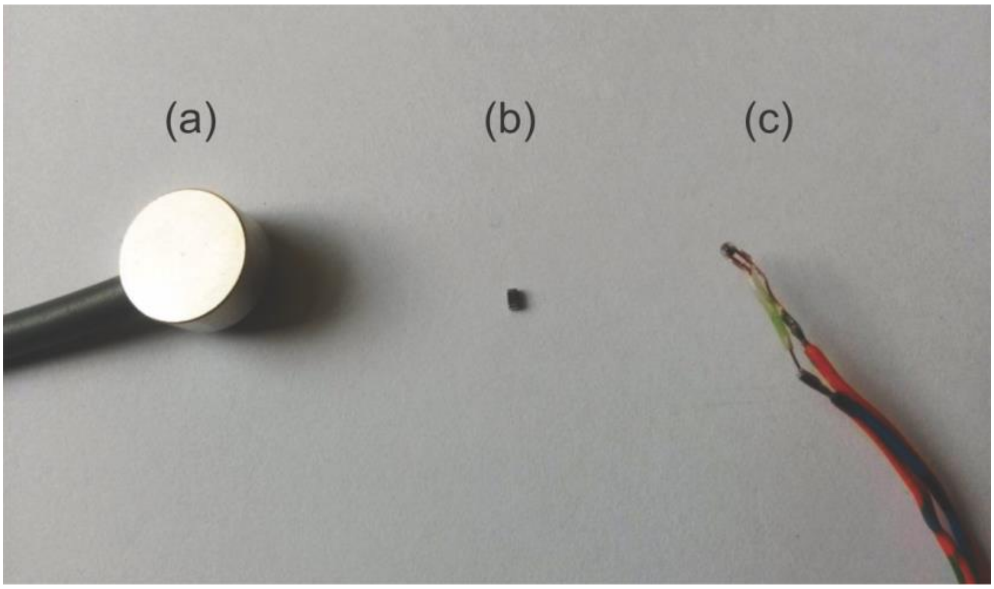

Figure 14 Tested thermistors: (a) thermistor enclosed in housing, (b) thermistor in bare SMD housing and (c) thermistor in a vacuum glass flask.

During the measurements we have found that the first thermistor has too much mass (due to the large housing) and therefore time constant of the temperature response was to large, effectively making the sensor to slow to track the temperature changes of the skin.

SMD thermistor has a poor signal-to-noise ratio. In spite of the electrical insulation and the use of shielding the sensor noise was too large. Additional electric insulation would only increase the time constant and the response of the sensor would be too slow. Best performance was achieved using a thermistor in a glass flask. Sensor in glass flask has low mass which allowed the sensor to respond very quickly to changes of skin temperature. The sensor also had the best signal-to-noise ratio. Based on the results of the comparison we have chosen the 62S3KF354G sensor from the Belatherm Company. Sensor was calibrated in the range of 25 ˚C to 45 ˚C in calibration chamber in the Laboratory for metrology and quality on the Faculty of Electrical Engineering. Figure 15 shows calibration results.

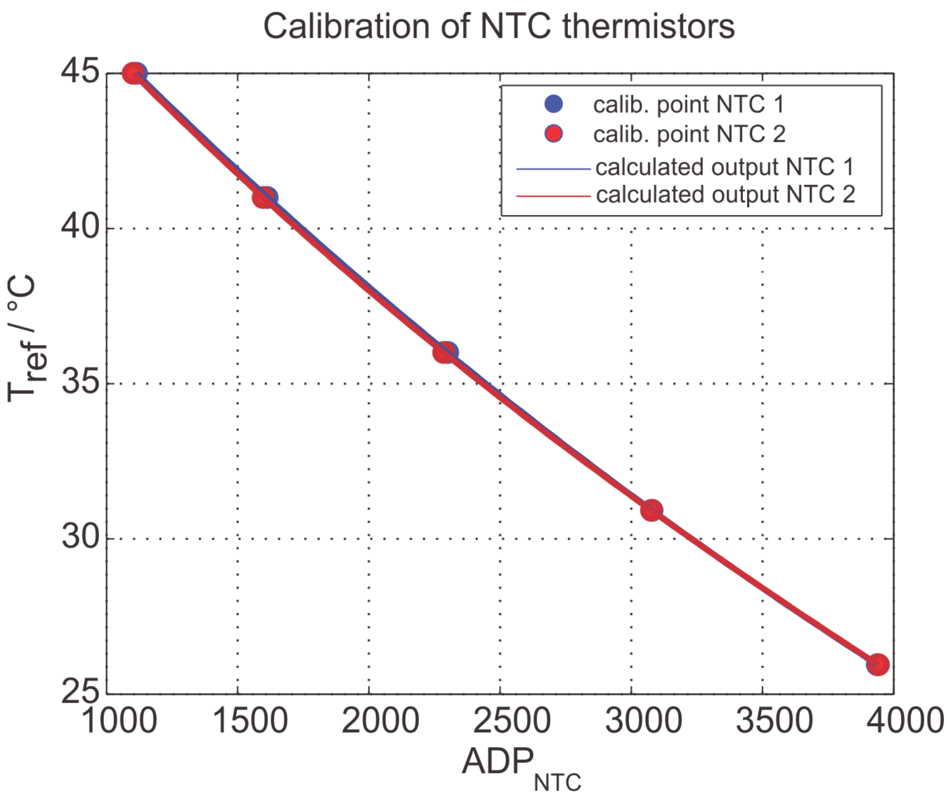

Figure 15 Calibration of NTC thermistors.

Sensor integration

Amplifiers for physiological signals were integrated into cylindrical handle and in spherical handle for measuring physiological parameters during the training with the robot. Analog amplifiers were integrated on a custom build PCB, while the ADC and communication protocols run on STM32F4 Discovery board. Signals were sent from Discovery board to serial port on a personal computer with frequency of 100 Hz. Signal processing was implemented using Matlab Simulink. Figure 16 shows both handles. Figure 17 shows sensor positions on the palm.

(a) (b)

Figure 16 Sensors integrated into (a) cylindrical handle and (b) spherical handle.

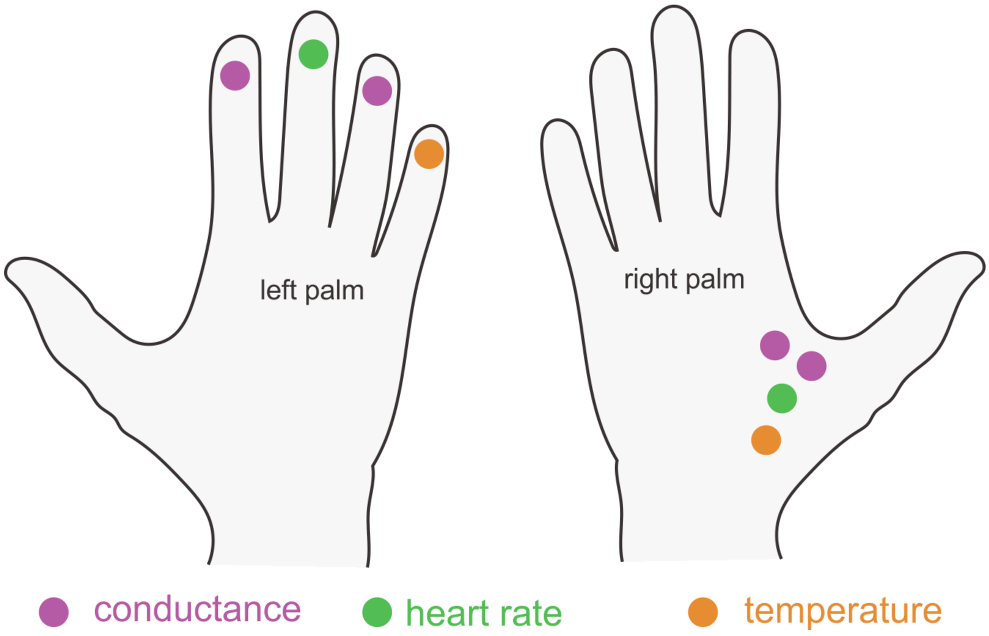

Figure 17 Electrode positions in handle and bracelet.

Experiments

Experiments were designed to test how well developed measurement system measures psychophysiological response of users during the training with the robot compared to the reference system. For reference system used was g.USBamp measuring system from Austrian company g.tec medical engineering, which has high resolution (24 bits) and a high sampling rate (up to 38.4 kHz) and is able to measure various physiological signals.

For the experiments we used haptic robot Haptic Master, which is equipped with a force sensor that measures the force in three axes. For the task in a virtual environment (Figure 18) we have developed a simulation of the inverted pendulum where the user needs to move the robot to stabilize the pendulum which is virtually attached to the end-point of the robot.

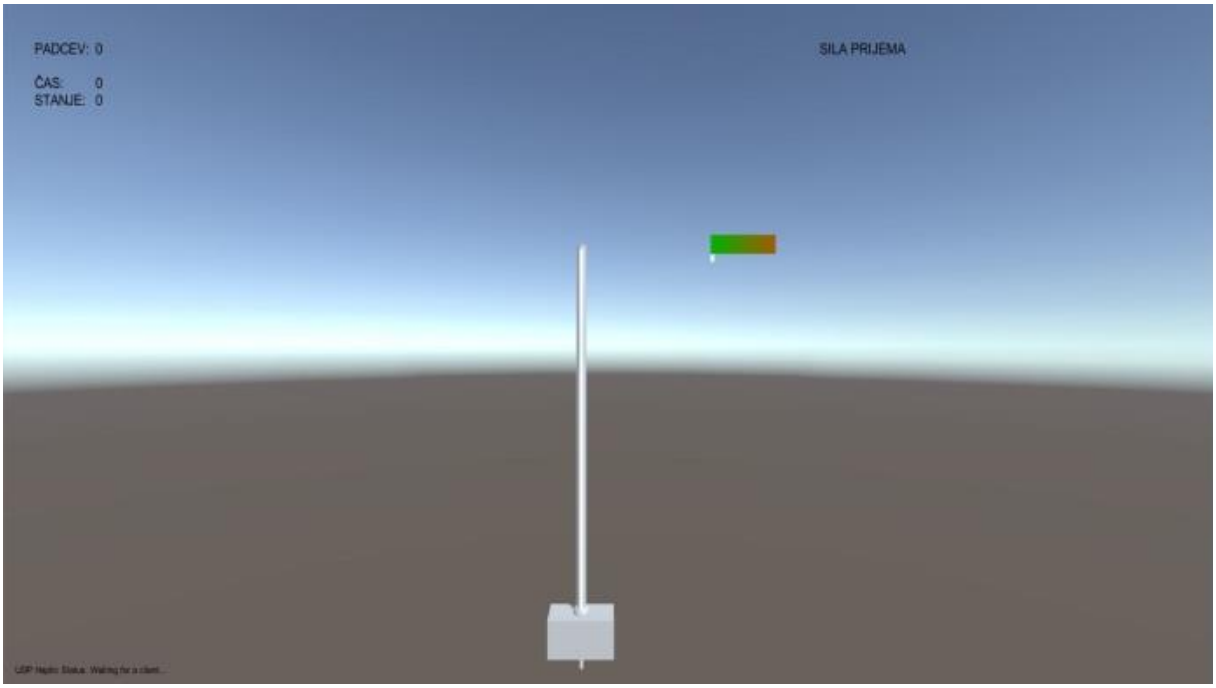

Figure 18 User graphical interface.

Full mathematical model of the inverted pendulum with haptic feedback was developed, so that we can adjust various parameters of the model (mass of the trolley, weight bars, damping carriage, damping rods and bars in length) while performing the task. Changing these parameters allows us to change the difficulty of the task.

$$\ddot{x} = \frac{F + \ddot{\vartheta} \cdot m \cdot l \cdot \cos\vartheta - \dot{\vartheta}^2 \cdot m \cdot l \cdot \sin\vartheta}{Mv + m} - B \cdot \dot{x}$$

$$\ddot{\vartheta} = \frac{-\ddot{x} \cdot \cos\vartheta + g \cdot \sin\vartheta - k \cdot \vartheta - b \cdot \dot{\vartheta}}{l}$$

Both handles can be attached to the robot in such a way that they have a freedom of rotation about a vertical axis. In this way we reduce the impact of motion artifacts on the quality of the signals. User grasps the handle with the fingertips positioned over the sensors, and moves the robot to perform the task. Sensory bracelet was attached on the right wrist, while a reference measurement system was attached on the tips of the fingers of the right hand. ECG measurements were done with adhesive electrodes with the reference measuring system that provides high-quality signals. Figure 19 shows the test subject while performing the task with attached sensors.

The task can be performed under various conditions: low cognitive challenge, high cognitive challenge, physical low challenge and physical high challenge. Due to motion artifacts we can assume that at high physical exertion the signal quality will be lower. Each measurement starts with an interval of sleep, we continue with the task interval and at the end repeat interval mode. In the sleep interval entity is released and is not communicating with the operator.

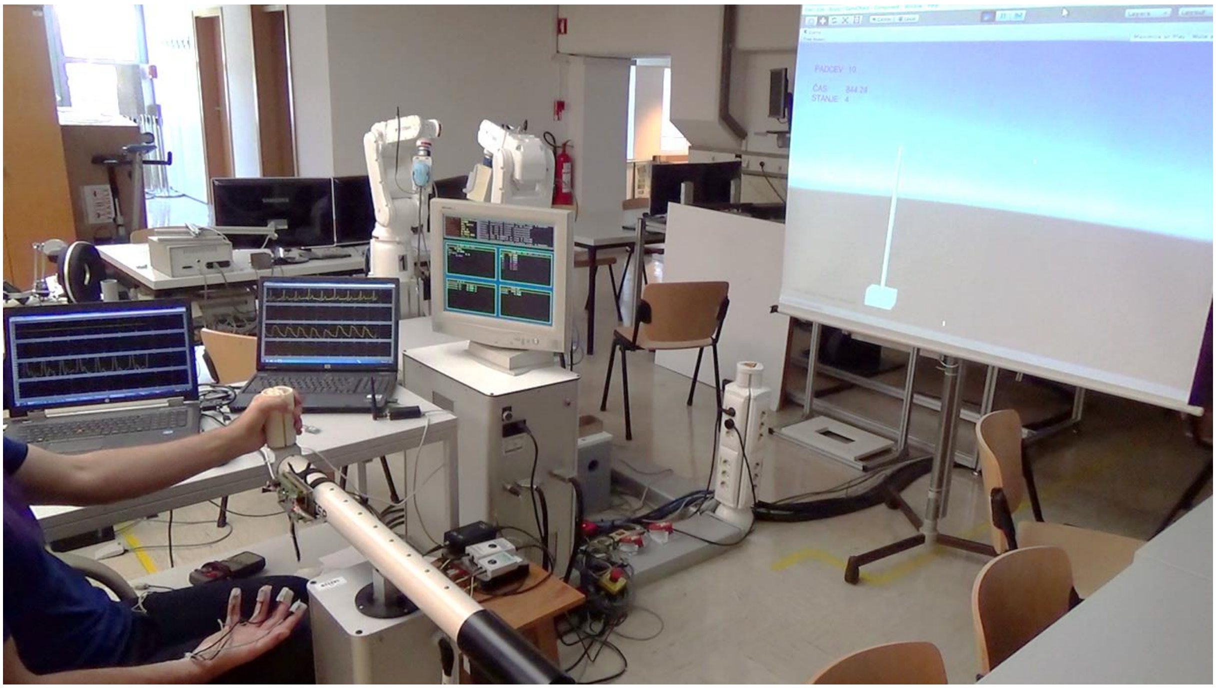

Figure 19 Experimental setup.

Signal preprocessing and feature extraction

Feature extraction in this case represents calculation of relevant features from the raw physiological signals. The ECG, for example, is a raw physiological signal from which mean heart rate or different measures of heart rate variability can be extracted. The following subsections describe the process of feature extraction for ECG, photoplethysmography, skin conductance and peripheral skin temperature.

Physiological features are generally calculated over an interval of fixed length, with lengths from a few seconds to a few minutes being common. In this study the interval length was two minutes. Shorter intervals were not used since some features require an interval of at least two minutes to be calculated (e.g. some measures of heart rate variability). Additionally, some signals such as peripheral skin temperature respond quite slowly to stimuli and cannot be properly evaluated over a short interval.

Electrocardiogram (ECG)

Of the three psychophysiological signals considered in the study, the ECG is the most complex to process. Many processing methods have been developed for other applications and can be used also in this case. The first step is to bandpass and high-pass filter the raw ECG to remove noise. For example, the 50 Hz notch filter reduces the power line interference. The fourth-order Butterworth high-pass filter with cutoff frequency 0.5 Hz was applied to reduce the baseline drift and noise caused by mechanical movement.

After filtering, R-peaks need to be detected in the ECG (Figure 20). R-peaks are the most prominent peaks in the ECG. Therefore, they are typically used as the basis for heart rate calculation. Numerous algorithms, mostly based on the amplitude or derivative of the filtered ECG, are available for R-peak detection, but a simple amplitude threshold followed by detection of signal peaks using the first (and second) derivative are usually sufficient.

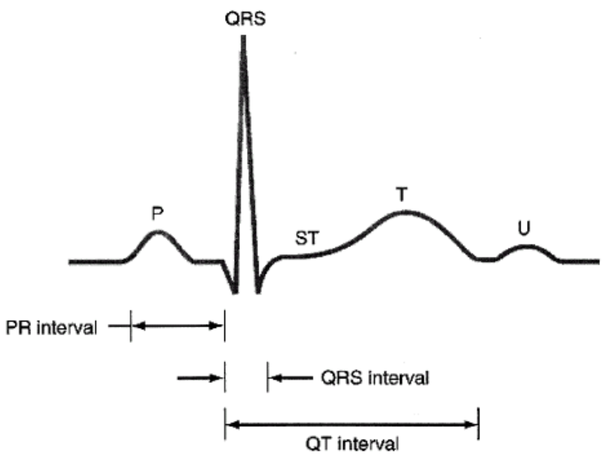

Figure 20 ECG signal

The time interval between two R-peaks is defined as a NN-interval (Figure 21). Heart rate is defined as the reciprocal value of the NN-interval. Mean heart rate is calculated for a specific time interval and is used as a primary ECG feature. Several standardized time- and frequency-domain measures of heart rate variability (HRV) can also be calculated, but might not be relevant in this case. The main reason for is the photoplethysmography (PPG) based measurement in low cost implementation of the sensory system. The PPG measurement enables reliable estimation of heart rate, while more complex measures of heart rate variability are sensitive to detection of peaks in the PPG signal. These other measures are typically calculated from the NN-intervals, which length is not reliably estimated from the PPG. For frequency-domain measures, NN-intervals are converted into a time series using cubic spline interpolation and the power spectral density of this time series is calculated using Welch's method of modified periodograms. The three time-domain features are the standard deviation of NN-intervals (SDNN), the square root of the mean squared differences of successive NN-intervals (RMSSD) and the percentage of interval differences of successive NN-intervals greater than 50 ms (pNN50). The power spectral density has two frequency bands which are typically of interest: the low-frequency band (LF) between 0.04 Hz and 0.15 Hz and the high-frequency band (HF) between 0.15 Hz and 0.4 Hz. Three frequency-domain HRV features were calculated: total power in the LF band, total power in the HF band (commonly referred to as respiratory sinus arrhythmia) and the ratio of the two (commonly referred to as the LF/HF ratio). These frequency-domain measures were calculated over a time period of two minutes.

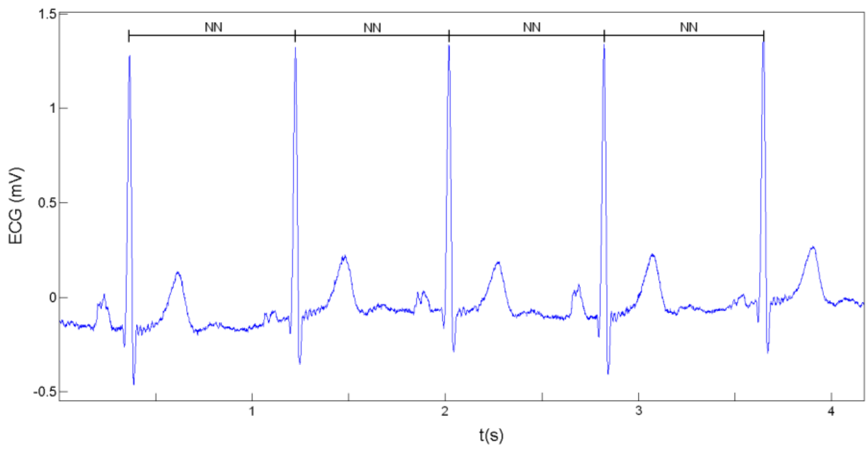

Figure 21 An example ECG signal with NN-intervals marked.

Photoplethysmography (PPG)

Figure 22 shows typical ECG and PPG outputs. Peaks in PPG measurements are not as pronounced as in the ECG signal. Nevertheless, the same methodology was used for the analysis of ECG and PPG. Method based on time derivatives of PPG signal was found robust enough (Figure 23).

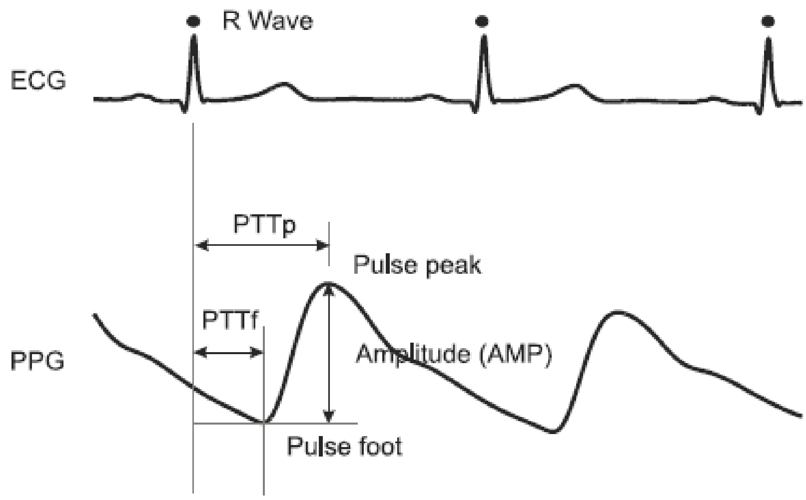

Figure 22 ECG and the corresponding PPG output

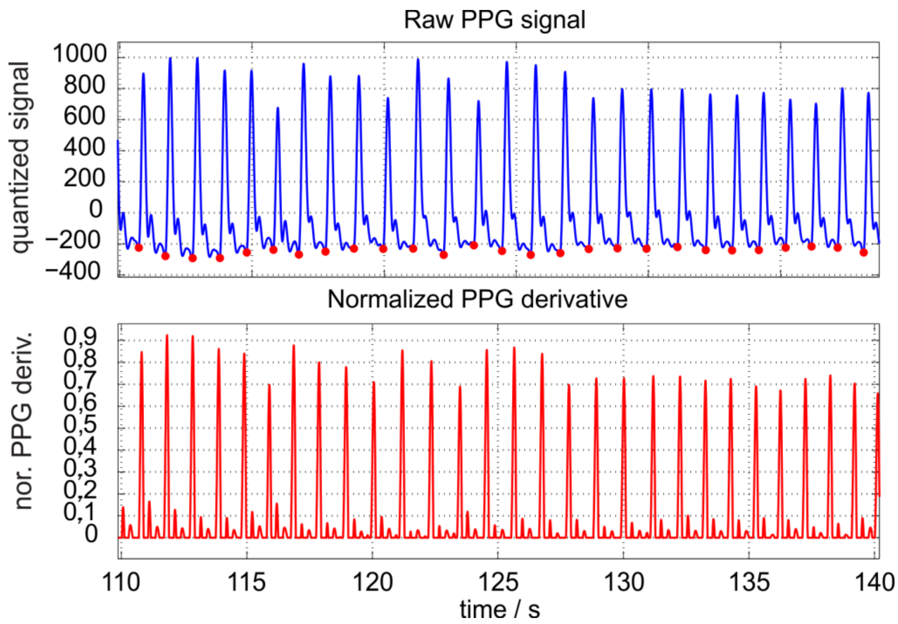

Figure 23 Processing of PPG signal

PPG signal can be significantly affected as a result of movement artifacts. In that case the above method for computation of heart rate is not adequate (Figure 24). In such case frequency domain analysis provides better results. Fast Fourier transform (FFT) was used to calculate amplitude spectrum of PPG signal. Heart rate was detected as the frequency value with the highest amplitude (Figure 25). The drawback of frequency domain analysis is the longer measurement interval (30 seconds typically) necessary to provide enough input data for FFT. Nevertheless, since 2-minute period was used for calculation of the mean heart rate, the FFT analysis does not affect the final result.

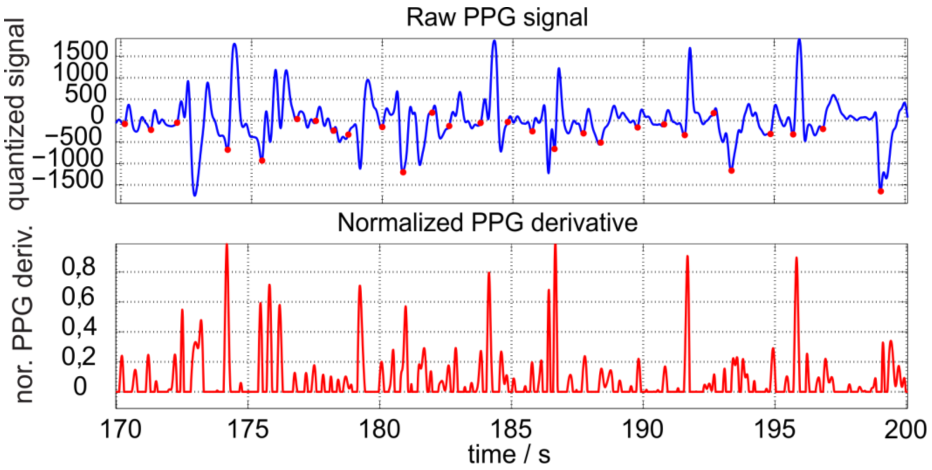

Figure 24 PPG signal affected by movement artifacts

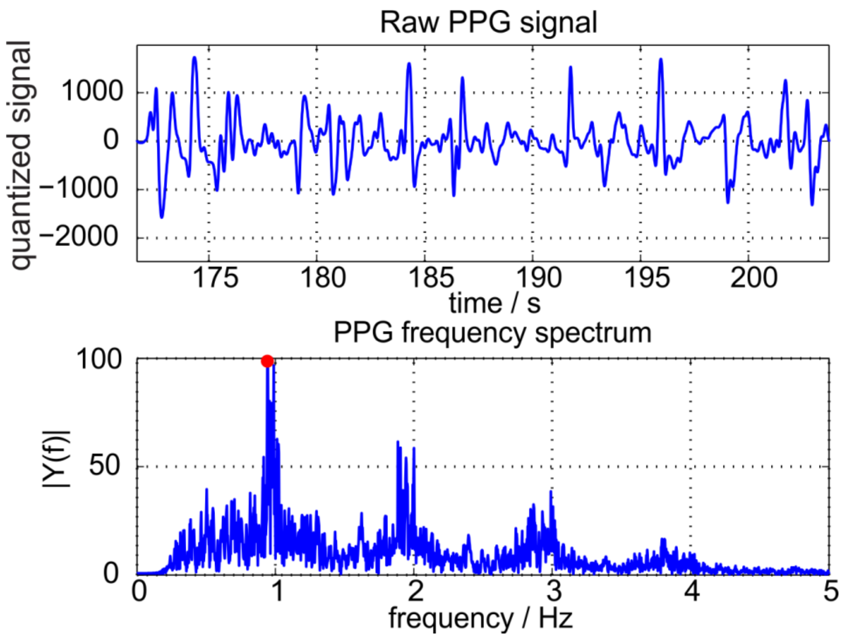

Figure 25 PPG analysis in frequency space

Skin conductance

An example of a skin conductance signal is shown in Figure 26. The two components of skin conductance are characterized as tonic and phasic (Figure 26). Tonic skin conductance is the slowly-changing baseline level of skin conductance, in the absence of any particular discrete environmental event, and is generally referred to as skin conductance level (SCL). Each person has a different SCL. Phasic skin conductance consists of rapid skin conductance increases followed by a return to the tonic level. These changes occur in response to discrete environmental stimuli, but can also occur spontaneously in the absence of any specific stimuli. These rapid increases are generally referred to as skin conductance responses (SCRs).

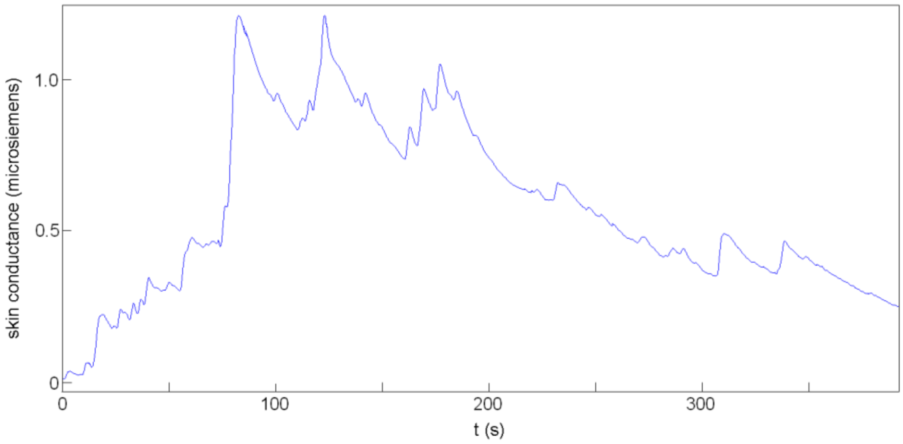

Figure 26 An example skin conductance signal with several skin conductance responses.

The skin conductance signal was first filtered with a fourth-order Butterworth low-pass filter with cutoff frequency set at 5 Hz for removal of high-frequency noise. Afterwards, two filters were separately applied to this signal to obtain tonic and phasic skin conductance. A fourth-order Butterworth low-pass filter with a cutoff frequency of 0.1 Hz was applied to the signal to obtain tonic skin conductance while a fourth-order Butterworth high-pass filter with a cutoff frequency of 0.1 Hz was applied to obtain phasic skin conductance. Mean SCL was calculated from tonic skin conductance. A transient increase in phasic skin conductance was detected as a SCR if its amplitude (from beginning of the increase to the peak) exceeded 0.05 microsiemens and its peak occurred less than 5 seconds after the beginning of the increase. SCR frequency and mean SCR amplitude were calculated.

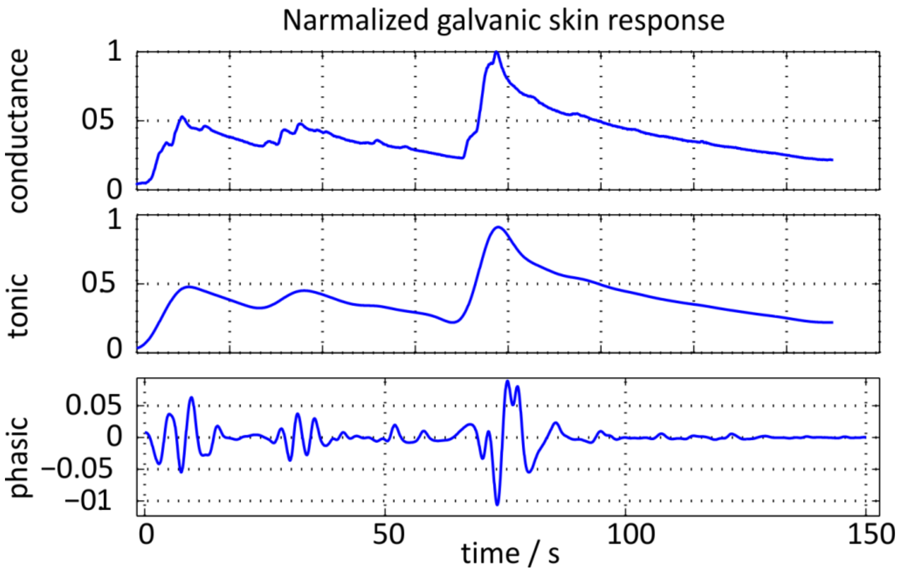

Figure 27 Galvanic skin response, tonic and phasic components

Peripheral skin temperature

Changes in peripheral skin temperature are caused by changes in the blood microcirculation, for example, at the fingers. Peripheral skin temperature changes very slowly compared to the other three physiological signals. Responses to stimuli begin to occur at more than 15 seconds after the stimulus (up to a minute after constant exposure to a stimulus and need an additional minute or two to reach the maximum deviation from the initial value). Because of this slowness, high-frequency noise was removed with a Butterworth fourth-order low-pass filter whose cut-off frequency was set at 1 Hz. The final skin temperature at the end of each period was calculated as the mean value over the last 5 seconds of the period. The final value rather than the mean value was chosen because of the slow, delayed response.

Results

The main focus of study was to investigate changes in physiological signals as a result of physical and mental effort during the execution of a task with a robot. At the same time we investigated performance of different prototypes for low-cost unobtrusive measurement of physiological signals.

Changes in physiological signals during exercise

Figure 28 shows typical responses of skin conductance and temperature during baseline and task. The two green areas indicate baseline measurements at the beginning and the end of the training session when the subject was comfortably resting.

The tonic component of skin conductance decreases during the baseline and increases during the task indicated with pink color in Figure 28. The same observation is valid also for phasic component of skin conductance that is indicated by the number of peaks superimposed on the tonic component. Thus, skin conductance can in general differentiate between resting and active involvement of the subject while performing robot supported training.

The peripheral skin temperature is much slower to respond compared to skin conductance. Results in Figure 28 indicate rising of peripheral skin temperature during resting (baseline) periods and decreasing temperature during the task. Since the task was physically not very demanding, the decrease of temperature during the active period is the result of mental activity that reduced the blood flow in the limbs to provide more energy to the brain. In the case of highly demanding physical task we would probably see an increase of peripheral temperature during the training due to the physical effort.

During the training positive changes of heart rate were also observed as demonstrated in Figure 29.

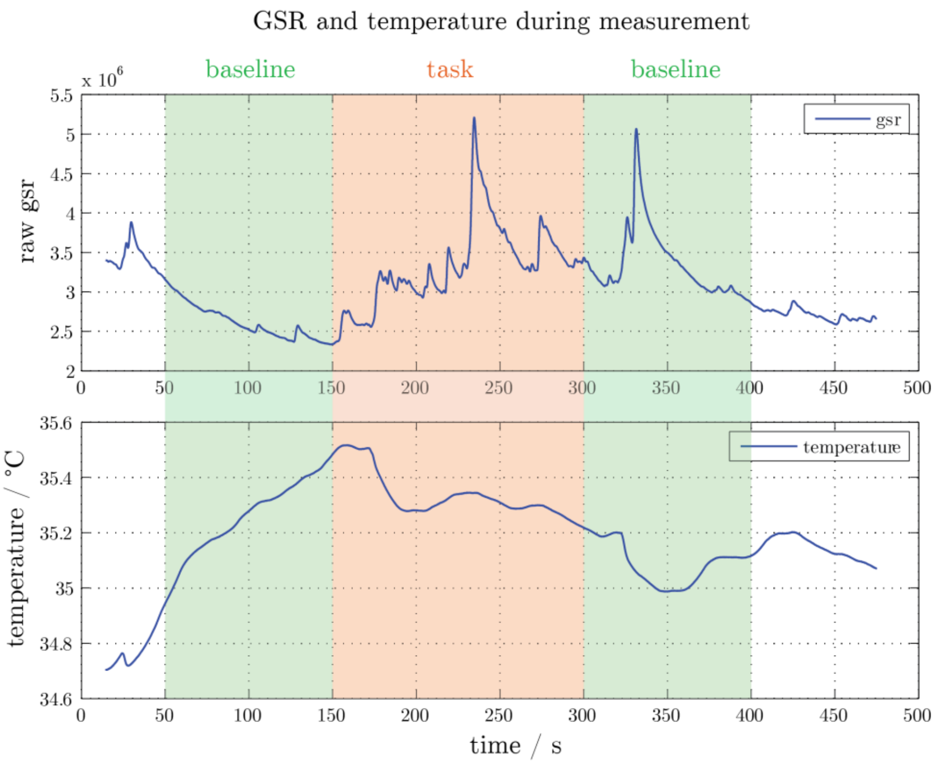

Figure 28 Skin conductance (above) and temperature (below) measured with g.tec in two resting periods (baseline, green) and task (pink)

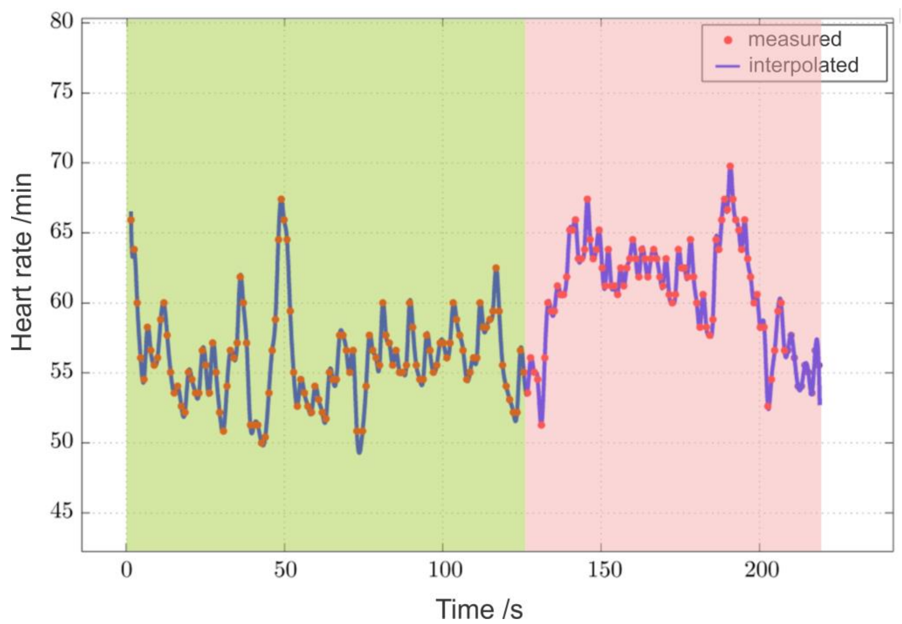

Figure 29 Heart rate measured with g.tec in a resting period (green) (baseline) and task (pink)

Comparison between different measurement systems

The observed changes in physiological signals during the robot-supported training are important. However, these changes are already well documented in the literature. What is more important is the possibility to measure these changes unobtrusively and with a low cost measurement system. This chapter summarizes the results of comparisons of different concepts for low-cost system and compares them to the reference high-end device. Different versions of the low-cost system were developed at different times and they cannot be used simultaneously during training with the robot (the subject can use only one type of handle at a time). Therefore, it was not possible to compare all systems during the same measurement sessions.

Figure 30 shows the heart rate measurement during the resting period (left) and the task (right). Three measurement concepts are compared: the reference measurement system, the handle and the bracelet. The ECG signal as measured by the g.tec system is not influenced by movement artifacts. The handle performs well during the baseline and also during the task if the subject pays attention to how it positions the fingers over the PPG sensor. However, in a typical task the PPG signal is highly distorted by movement artifacts as demonstrated in the right middle-row plot (with frequency analysis it is possible to estimate the heart rate also from this signal; however, a more robust measurement system would be preferable). Bracelet significantly outperformed the handle as it provided high quality signal during the resting period as well as during the task.

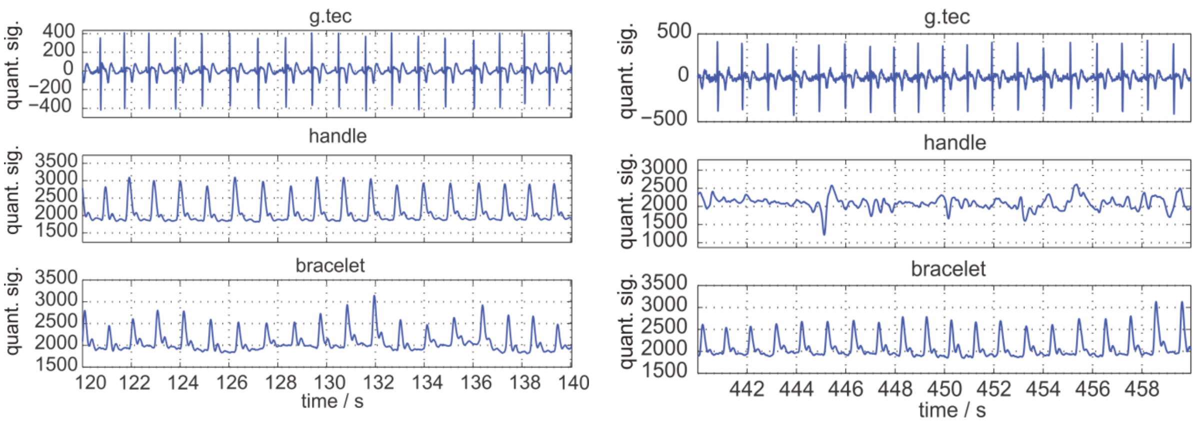

Figure 30 Heart rate measured with g.tec, handle and bracelet during the resting period (left) and task (right)

Figure 31 shows the skin conductance measurement during the resting period (left) and the task (right) for the same three concepts as above. The tonic component of skin conductance was measured reliably in resting and task condition with all three systems. Similar observation is also valid for the phasic component. However, the peaks of the phasic component are well visible on the signal from the reference measurement system; they are slightly small in the case of bracelet and even smaller on the handle. Thus, also in this case the configuration with the bracelet would be slightly preferable compared to the handle.

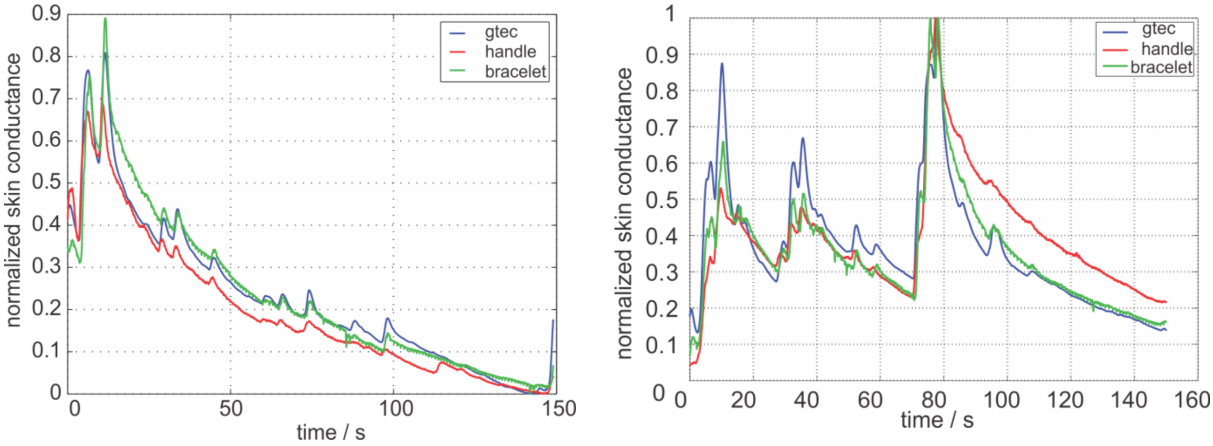

Figure 31 Skin conductance measured with g.tec, handle and bracelet during the resting period (left) and task (right)

Figure 31 shows the peripheral skin temperature measurement during the task for the same three concepts as above. The trends in the temperature are very similar. Since temperature sensors were calibrated, the measured values are valid. Slight differences may be the result of measurement in different positions on the body as well as the pressure that the subject applies on the temperature sensor during the arm movement. In terms of temperature measurement handle and bracelet perform adequately.

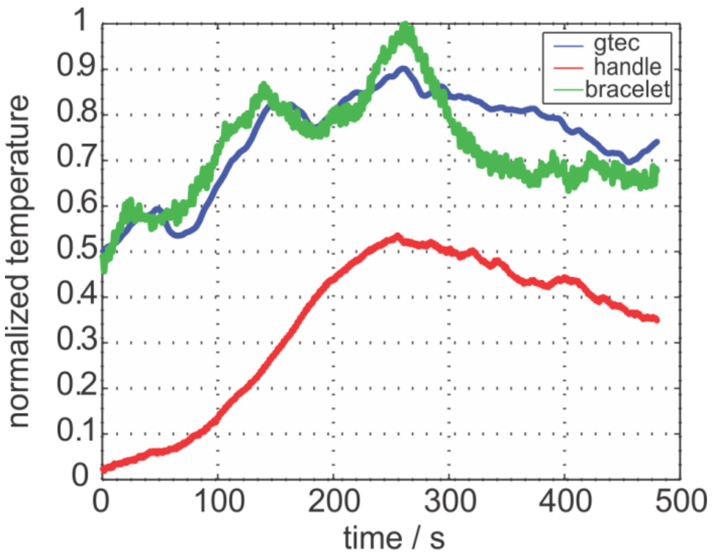

Figure 32 Peripheral temperature changes measured with g.tec, handle and bracelet during the task

The cylindrical-shape handle was found sensitive to movement artifacts. Namely, the subjects need to grasp the handle during the training and the grasp force is not constant due to the arm movement. From the perspective of motor training grasping is a desired feature of the rehabilitation device. However, from the measurement perspective this is not the most appropriate solution. Therefore, a hemispherical-shape handle was designed and is being evaluated. The advantage of such shape is that the hand is resting on the handle and does not generate excessive grasping force. Thus, measurements are less sensitive to movement artifacts. The first results with the hemispherical handle are promising, but more measurements are necessary and advantages/disadvantages of such configuration for training need to be evaluated.

In terms of heart rate (ECG) measurement a configuration that requires bimanual approach was also validated. In this case one ECG electrode is attached on the handle of the robot, while the other electrode is held by the other (free) hand. This configuration is typical for fitness devices where movement artifacts are pronounced. A low-cost bimanual ECG measurement system was developed and compared to the reference measurement system. The results of measurement during the task are summarized in Figure 33. The blue line indicates the reference measurement, the red-line signal is from the bimanual measurement, while the black line indicates the use of the reference electrode placed on the leg (signals are not synchronized). All three signals are of adequate quality to allow heart rate calculation as well as analysis of parameters based on the heart rate variability.

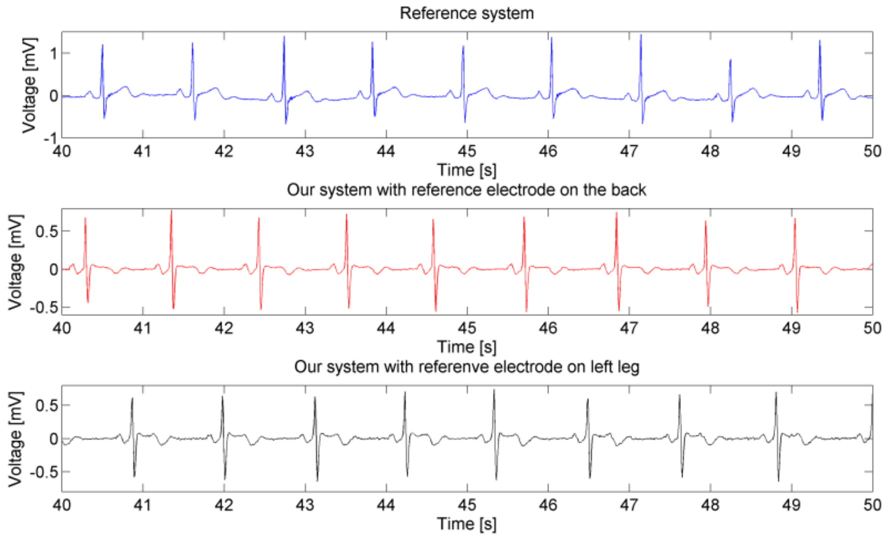

Figure 33 Non-synchronized ECG signals measured with g.tec (blue), bimanual measurement (red) and bimanual measurement with reference electrode on leg (black)

A more detailed analysis of changes of physiological signals during training is presented in Table 1. The results presented in the table summarize difference between the baseline and the task as well as differences between the reference and the low-cost measurement system for measuring physiological responses. Since most of the trials were performed with the cylindrical handle version of the low-cost system, results are presented only for this configuration. Nevertheless, based on the preliminary trials with the hemispherical version of the handle, the bracelet and the bimanual measurement of heart rate, we expect the results to additionally improve.

Most of the observed parameters change as a result of physical and mental activity during the task. A very important observation is that the low-cost measurement system performs adequately when compared to the reference measurement system. Especially the parameters based on ECG measurements are very well correlated. Somewhat unexpectedly also the parameters based on heart rate variability calculated from the PPG signal correspond to those computed from the reference system measurements. In terms of skin conductance similar trends were observed for both measurement systems, though detected changes are slightly different. The same observation is also valid for peripheral skin temperature.

Table 1 Analysis of physiological changes during baseline and task and comparison between reference and low-cost sensory system (handle version)

	HANDLE			REFERENCE		
	BASELINE	**TASK**	**RATIO**	**BASELINE**	**TASK**	**RATIO**
Heart rate						
Mean	63,910	66,749	4,443	63,874	66,737	4,482
Min	52,632	52,632	0,000	53,097	53,571	0,893
Max	81,081	76,923	-5,128	81,081	76,923	-5,128
SDNN	0,068	0,058	-14,543	0,067	0,057	-14,245
RMSSD	0,058	0,044	-23,157	0,057	0,042	-26,354
PNN50	0,313	0,201	-35,672	0,293	0,175	-40,063
HF	258,762	136,261	-47,341	234,567	117,128	-50,066
LF	2456,550	2884,367	17,415	2358,794	2825,311	19,778
LF/HF	9,493	21,168	122,974	10,056	24,121	139,873
Mean (from FFT)	61,890	66,650	7,692	61,890	66,650	7,692
Skin conductance						
Tonic (mean)	0,290	0,417	44,066	0,261	0,304	16,475
Tonic (final)	0,735	0,181	-75,337	0,868	0,043	-95,071
Phasic (final)	15,000	14,000	-6,667	15,000	15,000	0,000
Phasic (mean amp.)	0,047	0,050	6,658	0,080	0,080	-0,060
Phasic (stdv amp.)	0,039	0,045	17,399	0,092	0,094	2,037
TEMP						
Final	34,224	34,789	1,651	34,873	35,178	0,874

Conclusions

A proof-of concept system for validation of the low-cost sensory system and the patient model was developed and validated. In parallel with the system also prototypes of low-cost solutions for unobtrusive measurement of physiological signals were developed and compared to the reference measurements obtained from the g.tec high-end device. The following are the most important observations related to measurement of physiological signals:

1. The proposed one degree-of-freedom robotic device is suitable to elicit changes in subject's kinematics and dynamics as a result of movement (positions, velocities, accelerations, forces) as well as changes in physiological responses as a result of physical and mental activity.
2. The virtual environment combined with the robot results in detectable and repeatable changes in physiological signals.
3. The cylindrical-shape handle is adequate in terms of motor training and it also enables grasping force measurement; however, it is not the optimal solution in terms of physiological measurements.
4. The hemispherical-shape handle guarantees better results in terms of physiological measurements, since the hand is resting on the handle (not applying much force). However, such handle is not the most appropriate in terms of motor training as it does not stimulate grasping.
5. The ECG can be measured reliably in bimanual configuration, where one electrode is mounted on the robot handle, while the other electrode is placed in the resting hand of the exercising subject.
6. It is possible to conclude that the best solution would be a hemispherical-shape handle that would be held by the resting hand of the patient. The handle would provide a rest for the arm that is not exercising with the robot. This would eliminate movement artifacts. At the same time it would enable bimanual ECG measurement with the other electrode placed in the robot handle. Bimanual ECG measurement could be complemented with a PPG measurement on the resting hand. Another reason for this configuration would be the possibility to replace the robot handle with the Gloreha glove. And finally, providing a fix resting position for the arm that is not exercising would increase task performance by providing a reference coordinate system.

Literature on physiological sensors and sensor signal processing

1. A. Pantelopoulos, N.G. Bourbakis, "A Survey on Wearable Sensor-Based Systems for Health Monitoring and Prognosis," *IEEE Transactions on Systems, Man, and Cybernetics, Part C: Applications and Reviews*, vol.40, no.1, pp. 1-12, 2010.
2. R. Paradiso, G. Loriga, N. Taccini, "A wearable health care system based on knitted integrated sensors," *IEEE Transactions on Information Technology in Biomedicine,* vol.9, no.3, pp.337,344, 2005.
3. C.W. Mundt, K.N. Montgomery, U.E. Udoh, V.N. Barker, G.C. Thonier, A.M. Tellier, R.D. Ricks, R.B. Darling, Y.D. Cagle, N.A. Cabrol, S.J. Ruoss, J.L. Swain, J.W. Hines, G.T. Kovacs, "A multiparameter wearable physiologic monitoring system for space and terrestrial applications," *IEEE Trans Inf Technol Biomed*, vol. 9, no. 3, pp.382-91, 2005.
4. S. Patel, H. Park, P. Bonato, L. Chan, M. Rodgers, "A review of wearable sensors and systems with application in rehabilitation," *Journal of NeuroEngineering and Rehabilitation*, vol. 9, no. 21, 2012.
5. P.S. Pandian, K. Mohanavelu, K.P. Safeer, T.M. Kotresh, D.T. Shakunthala, Parvati Gopal, V.C. Padaki, "Smart Vest: Wearable multi-parameter remote physiological monitoring system," *Medical Engineering & Physics*, vol. 30, pp. 466–477, 2008.
6. P. Ming-Zher, N.C. Swenson, R.W. Picard, "A Wearable Sensor for Unobtrusive, Long-Term Assessment of Electrodermal Activity," *IEEE Transactions on Biomedical Engineering*, vol.57, no.5, pp.1243,1252, 2010.
7. D. Novak, A. Nagle, U. Keller and R. Riener, "Increasing motivation in robot-aided arm rehabilitation with competitive and cooperative gameplay," *Journal of NeuroEngineering and Rehabilitation*, vol. 11, no. 64, 2014.
8. D. Novak, B. Beyeler, X. Omlin and R. Riener, "Workload estimation in physical human-robot interaction using physiological measurements," *Interacting with Computers*, pp. 1-14, 2014.
9. D. Novak, A. Nagle and R. Riener, "Linking recognition accuracy and user experience in an affective feedback loop," *IEEE Transactions on Affective Computing*, 2014, vol. 5, no. 2, pp. 168-172, 2014.
10. J. Ogorevc, G. Geršak, D. Novak and J. Drnovšek, "Metrological evaluation of skin conductance measurements," *Measurement*, vol. 46, pp. 2993-3001, 2013.
11. D. Novak, M. Mihelj and M. Munih, "A survey of methods for data fusion and system adaptation using autonomic nervous system responses in physiological computing," *Interacting with Computers*, vol. 24, pp. 154-172, 2012.
12. D. Novak, M. Mihelj and M. Munih, "Dual-task performance in multimodal human-computer interaction: a psychophysiological perspective," *Multimedia Tools and Applications*, vol. 56, pp. 553-567, 2012.
13. M. Mihelj, D. Novak, M. Milavec, J. Ziherl, A. Olenšek and M. Munih, "Virtual rehabilitation environment using principles of intrinsic motivation and game design," *Presence: Teleoperators and Virtual Environments*, vol. 21, pp. 1-15, 2012.

14. D. Novak, M. Mihelj, J. Ziherl, A. Olenšek and M. Munih, “Psychophysiological measurements in a biocooperative feedback loop for upper extremity rehabilitation,” *IEEE Transactions on Neural Systems and Rehabilitation Engineering*, vol. 19, pp. 400-410, 2011.
15. D. Novak, M. Mihelj and M. Munih, “Psychophysiological responses to different levels of cognitive and physical workload in haptic interaction,” *Robotica*, vol. 29, pp. 367-374, 2011.
16. Koenig, D. Novak, X. Omlin, M. Pulfer, E. Perreault, L. Zimmerli, M. Mihelj and R. Riener, “Real-time closed-loop control of cognitive load in neurological patients during robot-assisted gait training,” *IEEE Transactions on Neural Systems and Rehabilitation Engineering*, vol. 19, pp. 453-464, 2011.
17. D. Novak, J. Ziherl, A. Olenšek, M. Milavec, J. Podobnik, M. Mihelj and M. Munih, “Psychophysiological responses to robotic rehabilitation tasks in stroke,” *IEEE Transactions on Neural Systems and Rehabilitation Engineering*, vol. 18, pp. 351-361, 2010.
18. J. Ziherl, D. Novak, A. Olenšek, M. Mihelj and M. Munih, “Evaluation of upper extremity robot-assistances in subacute and chronic stroke subjects,” *Journal of NeuroEngineering and Rehabilitation*, vol. 7, no. 52, 2010.
19. D. Novak, *Adaptive integration of psychophysiological variables for robotic training : doctoral dissertation*. Ljubljana
20. M.-Z. Poh, N. C. Swenson and R. W. Picard, "*A wearable sensor for unobtrusive, long-term assessment of electrodermal activity*," IEEE Transactions on Biomedical Engineering, vol. 57, no. 5, pp. 1243-1252, 2010.
21. D. C. Fowles, M. J. Christie, R. Edelberg, W. W. Grings, D. T. Lykken and P. H. Venables, "*Publication recommendations for electrodermal measurements*," Psychophysiology, vol. 18, no. 3, pp. 232-239, 1981.